JACS
JOURNAL OF THE AMERICAN CHEMICAL SOCIETY
Article
pubs.acs.org/JACS

Cobalt-Catalyzed C(sp^2)-H Borylation: Mechanistic Insights Inspire Catalyst Design

Jennifer V. Obligacion, Scott P. Semproni, Iraklis Pappas, and Paul J. Chirik*

Department of Chemistry, Princeton University, Princeton, New Jersey 08544, United States

Supporting Information

ABSTRACT: A comprehensive study into the mechanism of bis(phosphino)pyridine (PNP) cobalt-catalyzed C−H borylation of 2,6-lutidine using B_2Pin_2 (Pin = pinacolate) has been conducted. The experimentally observed rate law, deuterium kinetic isotope effects, and identification of the catalyst resting state support turnover limiting C−H activation from a fully characterized cobalt(I) boryl intermediate. Monitoring the catalytic reaction as a function of time revealed that borylation of the 4-position of the pincer in the cobalt catalyst was faster than arene borylation. Cyclic voltammetry established the electron withdrawing influence of 4-BPin, which slows the rate of C−H oxidative addition and hence overall catalytic turnover. This mechanistic insight inspired the next generation of 4-substituted PNP cobalt catalysts with electron donating and sterically blocking methyl and pyrrolidinyl substituents that exhibited increased activity for the C−H borylation of unactivated arenes. The rationally designed catalysts promote effective turnover with stoichiometric quantities of arene substrate and B_2Pin_2. Kinetic studies on the improved catalyst, **4-(H)$_2$BPin**, established a change in turnover limiting step from C−H oxidative addition to C−B reductive elimination. The iridium congener of the optimized cobalt catalyst, **6-(H)$_2$BPin**, was prepared and crystallographically characterized and proved inactive for C−H borylation, a result of the high kinetic barrier for reductive elimination from octahedral Ir(III) complexes.

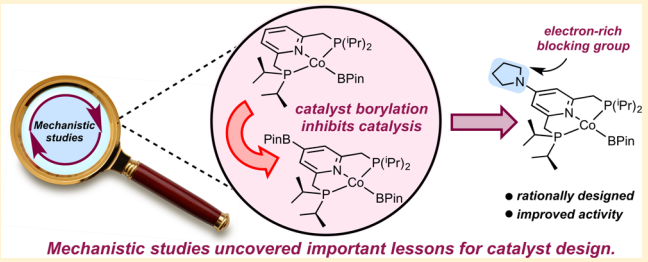

INTRODUCTION

The direct functionalization of carbon−hydrogen bonds has emerged as a powerful tool in organic synthesis.[1] Among the many methods now available, transition metal catalyzed arene C−H borylation[2] has emerged as one of the most widely applied, a result of the value and versatility of the resulting organoboron products,[3] particularly as the nucleophilic partners in C−C and C−N cross coupling reactions.[4] C−H borylation is also attractive due to its highly predictable site selectivity that is governed by steric accessibility and C−H bond acidity rather than relying on directing functionality for substrate-catalyst preorganization.

Among precious metal C−H borylation catalysts, iridium phosphine[5] and bipyridine[6] complexes have emerged as the most effective due to their high activity and ease of use. The functional group compatibility of this family of catalysts has enabled optimization by high throughput experimentation[7] as well as application to the elaboration of complex heterocycles[8] and late stage intermediates in the context of total synthesis.[9] Supported rhodium and iridium complexes have also been discovered that complement the reactivity and selectivity of the soluble organometallic compounds.[10]

Extensive experimental mechanistic investigations[11] as well as computational studies[12] on the [Ir(dtbpy) (BPin)$_3$(COE)] (COE = cyclooctene; dtbpy = 4,4′-di-*tert*-butyl-2,2′-bipyridine; Pin = pinacolate) catalyst support an Ir(III)−Ir(V) redox couple where Ir^{III}(dtbpy) (BPin)$_3$ promotes rate-determining C−H bond cleavage.[11] Reductive elimination of the carbon−boron bond liberates the arylboronate ester product and catalyst regeneration occurs by oxidative addition of B_2Pin_2 (Scheme 1).

The potential economic and environmental advantages associated with earth abundant transition metals such as iron, cobalt and nickel has motivated interest in developing first row transition metal catalysts for C−H borylation.[13] These metals also offer the opportunity for new reactivity, selectivity and

Scheme 1. Accepted Mechanism for Iridium-Catalyzed C−H Borylation[11,12a]

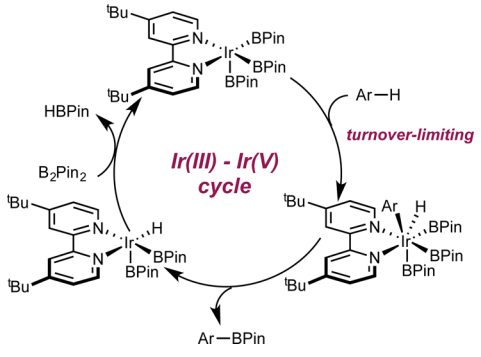

Received: June 14, 2016
Published: July 31, 2016

DOI: 10.1021/jacs.6b06144
J. Am. Chem. Soc. 2016, 138, 10645−10653

possibly functional group tolerance due to increased ligand substitutional lability and kinetically and thermodynamically accessible oxidation states separated by one electron.[14] A seminal report on stoichiometric C−H borylation was reported by Hartwig and co-workers with first row transition metals with the UV activation of Fp(BCat) (Fp = $[(\eta^5\text{-}C_5H_5)Fe(CO)_2]$; Cat = catecholate) to promote C−B bond formation with arenes.[15] Mankad and co-workers recently reported a catalytic variant of this process where metal−metal cooperativity was used as a strategy to enable turnover.[16] Irradiation of a benzene-d_6 solution containing HBPin and 5 mol % of (IPr)CuFp (IPr = *N*,*N*-bis(2,6-diisopropylphenyl)imidazole-2-ylidene) produced C_6D_5BPin in >70% yield. Control experiments established the necessity of a polar metal−metal bond in the heterobimetallic precursor for catalysis.[13,17] Cyclopentadienyl iron carbene[18] and bisphosphine[19] complexes, Fe_2O_3 nanoparticles[20] as well as Ni complexes[21] have also been reported for catalytic C−H borylation although in many cases substrate scope is limited to selected arenes or heteroarenes.

Our laboratory has recently reported that several classes of cobalt complexes supported by tridentate pincer-type ligands are effective for the C−H borylation of five-membered heteroarenes, substituted pyridines and arenes using either HBPin or B_2Pin_2 as the boron source.[22,23] Among these, the bis(phosphine)pyridine pincer complexes, (^{iPr}PNP)CoR (R = alkyl)[24] have proven the most active and synthetically useful (Scheme 2).[22] Up to 5000 turnovers have been observed for

Scheme 2. Examples of Catalytic C−H Borylation Promoted by (^{iPr}PNP)CoCH$_2$SiMe$_3$ (1-CH$_2$SiMe$_3$)[22]

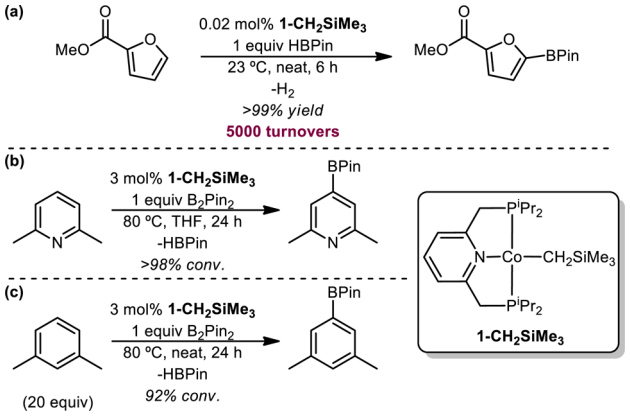

the borylation of methyl furan-2-carboxylate at 23 °C (Scheme 2a). High *ortho* selectivity for the borylation of fluorobenzene and synthesis of selected 2-borylpyridine derivatives illustrate some of the reactivity and selectivity enabled by cobalt that is distinct from known precious metal catalysts. For unactivated arenes such as toluene and *meta*-xylene, a 20-fold excess of substrate was required for reasonable turnover (Scheme 2c) and highlights the need for next generation catalysts with improved activity.

Understanding the mechanism of cobalt-catalyzed C−H borylation is therefore of interest for rational catalyst design. Open questions include (i) what redox couple is operative during cobalt-catalyzed C−H borylation, (ii) what is the identity of the compound responsible for C−H activation, and (iii) what is the turnover-limiting step during the catalytic cycle? Stoichiometric studies with (^{R}PNP)CoR′ have demonstrated that the pincer ligand generates a sufficiently electron rich cobalt center to promote the two-electron oxidative addition of H−H, C−X, and C−H bonds[25] but the role of this fundamental transformation and its relative rate to other elementary steps has yet to be firmly established in the context of catalytic C−H borylation.

Here we describe a comprehensive investigation into the mechanism of cobalt-catalyzed arene C−H borylation and establish a catalytic cycle that operates via a Co(I)−Co(III) redox couple. The nature of the cobalt(I) complex responsible for C−H activation is also identified as is competing borylation of the cobalt catalyst that is responsible for its inhibition during the course of turnover. These findings provided insight for the synthesis of the next generation C−H borylation catalysts with improved activity.

RESULTS AND DISCUSSION

The cobalt(III) dihydride boryl, *trans*-(^{iPr}PNP)Co(H)$_2$BPin (**1-(H)$_2$BPin**) was previously identified as the catalyst resting state during the borylation of 2-methylfuran with HBPin at 23 °C, suggesting a Co(I)−Co(III) redox couple during catalysis.[22] While HBPin proved effective for the Co-catalyzed borylation of five-membered heterocycles, it was ineffective for pyridines and unactivated arenes. These substrates required B_2Pin_2 for synthetically useful yields. To understand the origin of this difference in reactivity and likely different mechanism for turnover, more detailed studies were conducted on the cobalt-catalyzed borylation of 2,6-lutidine using B_2Pin_2. This specific heteroarene was selected for these studies due to the formation of a single borylated product, facilitating product characterization.

Determination of the Rate Law. The experimental rate law for the borylation 2,6-lutidine with B_2Pin_2 was determined at 80 °C using the method of initial rates (up to 10% conversion) with **1-CH$_2$SiMe$_3$** as the precatalyst. Measurements were made with varying concentrations of 2,6-lutidine, B_2Pin_2 and **1-CH$_2$SiMe$_3$** and the results of these studies are reported in Table S2. These data established the following overall rate equation:

$$\text{rate} = k_{obs}[\textbf{1-CH}_2\textbf{SiMe}_3]^1[\text{2, 6-lutidine}]^1[B_2Pin_2]^0 \quad (1)$$

Measurement of Deuterium Kinetic Isotope Effects (KIE). Using 3 mol % of **1-CH$_2$SiMe$_3$** as the precatalyst and B_2Pin_2 as the boron source, a kinetic isotope effect (KIE) of 2.9(1) was measured for the borylation of 2,6-lutidine and 4-*d*-2,6-lutidine at 80 °C by comparison of relative initial rates determined in two separate vessels (see Table S7). Observation of a normal, primary KIE of this magnitude also supports turnover limiting C−H activation, similar to the primary KIE value of 3.3(6) for two separate borylation reactions of 1,2-dichlorobenzene and 1,2-dichlorobenzene-d_4 for iridium catalysts.[11]

Determination of the Catalyst Resting State as a Function of Time. The catalytic C−H borylation of 2,6-lutidine with B_2Pin_2 and 10 mol % of **1-CH$_2$SiMe$_3$** at 80 °C was monitored by ^{1}H and ^{31}P NMR spectroscopies in THF-d_8 at 23 °C to gain insight into the identity of the cobalt compound present during turnover (see S18 for complete experimental details). A higher catalyst loading of 10 mol % (in contrast to 3 mol % communicated previously[22]) was used to facilitate observation of the cobalt compounds present in solution. After both 5 min and 1 h of heating at 80 °C, corresponding to <5 and 27% yields of products respectively, a single diamagnetic

DOI: 10.1021/jacs.6b06144
J. Am. Chem. Soc. 2016, 138, 10645−10653

cobalt compound (**A**) was observed. The ^{31}P NMR spectrum at 23 °C exhibits a single peak centered at 56.25 ppm, diagnostic of a Co(I) compound.[25] At 5 h of reaction time, corresponding to 65% yield of product, **A** and another cobalt compound (**B**) with a ^{31}P NMR signal (23 °C) at 93.88 ppm were observed. After 10 h at 80 °C (85% yield of product), **B** became the cobalt species present in the highest concentration (Figure 1).

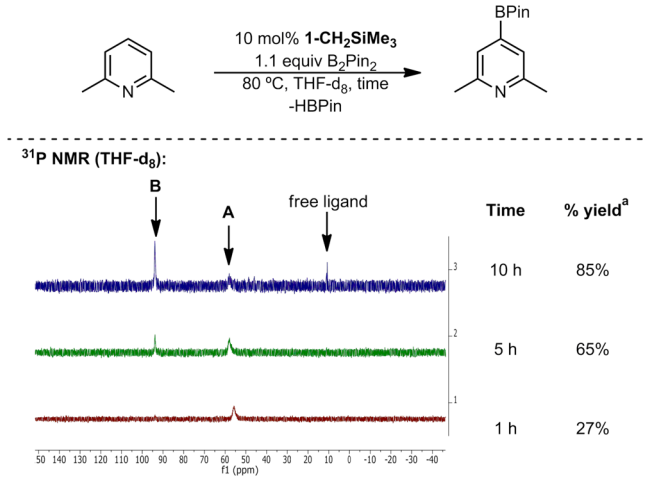

Figure 1. ^{31}P NMR spectrum (at 23 °C) of the reaction mixture of 2,6-lutidine and B_2Pin_2 in the presence of 10 mol % of **1-CH$_2$SiMe$_3$** in THF-d_8 at 80 °C. [a]NMR yield of product.

Identification of A and B. A series of stoichiometric experiments were conducted using **1-CH$_2$SiMe$_3$** as the starting cobalt complex to determine the identities of **A** and **B** (Scheme 3). Addition of one equivalent of B_2Pin_2 to a benzene-d_6 or

Scheme 3. Stoichiometric Reactions on 1-CH$_2$SiMe$_3$

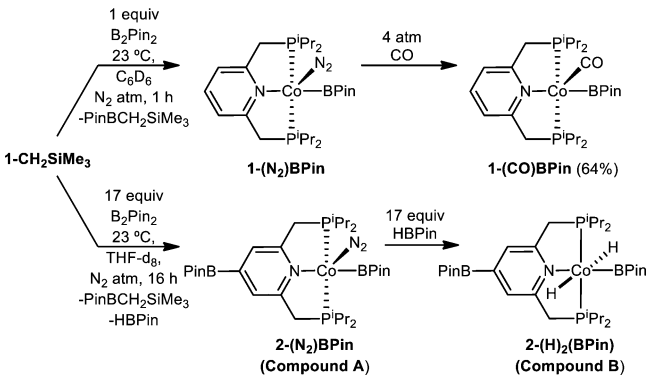

THF-d_8 solution of **1-CH$_2$SiMe$_3$** resulted in formation of Me_3SiCH_2BPin along with a new diamagnetic cobalt complex identified as **1-(N$_2$)BPin**, over the course of 1 h at 23 °C. A strong N−N band was observed at 2055 cm^{-1} in the benzene-d_6 solution infrared spectrum of the compound, confirming dinitrogen coordination. The benzene-d_6 ^{1}H NMR spectrum of **1-(N$_2$)BPin** exhibited broadened resonances at 23 °C, likely a result of reversible N_2 coordination in solution. Unfortunately this compound was only observed in solution as attempts to isolate it in the solid state either by recrystallization or removal of the solvent in vacuo resulted in decomposition.

To obtain an isolable variant of **1-(N$_2$)BPin**, replacement of the labile N_2 ligand with a stronger π-acidic ligand was explored. Addition of 4 atm of CO to a benzene-d_6 solution of the compound instantly afforded a new, diamagnetic C_s symmetric cobalt complex identified as **1-(CO)BPin** (Scheme 3). Recrystallization from diethyl ether at −35 °C produced blue-purple crystals suitable for X-ray diffraction in 64% yield (see Figure 2). The geometry about the metal center is best described as pseudo trigonal bipyramidal, with the carbonyl and phosphine ligands occupying the equatorial positions, and the boryl and pyridine ligands occupying the axial positions. The P−Co−P and N_{py}−Co−B angles of 139.68(2)° and 167.29(7)°, respectively, support this geometry. The IR spectrum of **1-(CO)BPin** in KBr displayed a single intense band at 1854 cm^{-1}, consistent with a metal−carbonyl stretching mode. Unlike **1-(N$_2$)BPin**, **1-(CO)BPin** was stable in benzene-d_6 solution and in the solid state for extended periods.

The THF-d_8 ^{31}P NMR spectrum of **1-(N$_2$)BPin** exhibited a single peak at 56.28 ppm, similar to the value of 56.25 ppm observed for **A**. However, the ^{1}H NMR spectra of **1-(N$_2$)BPin** and **A** are distinct. For example, **A** exhibits a singlet at 6.50 ppm, assigned as the proton in the 3-position of the pyridine in the PNP pincer. The collapse of the doublet normally observed for this hydrogen, for example in **1-(N$_2$)BPin**, signals modification of the 4-position of the chelate, likely by C−H borylation. Treatment of **1-CH$_2$SiMe$_3$** with excess B_2Pin_2 (Scheme 3) in THF-d_8 resulted in formation of a new diamagnetic cobalt compound over the course 16 h at 23 °C. Notably, a new singlet was observed at 6.50 ppm, identical that observed with **A**. Unlike **1-(N$_2$)BPin**, this compound proved stable in THF-d_8 and fully characterized by multinuclear and 2-D NMR spectroscopy. The NMR data, along with observation of a strong N−N band at 2065 cm^{-1} in the KBr IR spectrum, established the identity of this compound as the borylated cobalt(I)-boryl complex, **2-(N$_2$)BPin**. This compound is also intermediate **A** formed during catalytic borylation of 2,6-lutidine.

Experiments were also conducted to determine the identity of **B**. The ^{1}H NMR spectrum of this compound also exhibited a singlet at 6.82 ppm, signaling modification of the 4-position of the pyridine ring of the chelate. Addition of excess HBPin to a THF-d_8 solution of **2-(N$_2$)BPin** at 23 °C generated a diamagnetic cobalt product with identical spectroscopic properties as **B**, which was identified as **2-(H)$_2$BPin**. This compound was independently synthesized by the addition of 2 equiv of HBPin to **2-CH$_3$** (see Scheme 5) and characterized by X-ray diffraction (Scheme 4).

Proposed Mechanism. Having established the turnover-limiting step from the kinetic data and identified the catalyst resting states as a function of time, the experimental data support the reaction mechanism proposed in Scheme 4. Catalyst initiation occurs by the reaction of **1-CH$_2$SiMe$_3$** with B_2Pin_2 under an N_2 atmosphere to generate **1-(N$_2$)BPin** with the concomitant release of Me_3SiCH_2BPin (step 1). Borylation of the catalyst with B_2Pin_2 generates catalyst resting state 1 at 23 °C, **2-(N$_2$)BPin** and HBPin (step 2). Following N_2 dissociation (step 3), the cobalt(I) boryl intermediate undergoes turnover-limiting C−H oxidative addition to generate a cobalt(III) hydride boryl aryl intermediate (step 4). This is followed by reductive elimination to form the arylboronate ester product and a cobalt(I) hydride (step 5). Oxidative addition of B_2Pin_2 (step 6) and reductive elimination of HBPin (step 7) completes the catalytic cycle. At higher conversions when the C−H borylation reaction generates a substantial amount of HBPin, the cobalt(I) hydride species undergoes

DOI: 10.1021/jacs.6b06144
J. Am. Chem. Soc. 2016, 138, 10645−10653

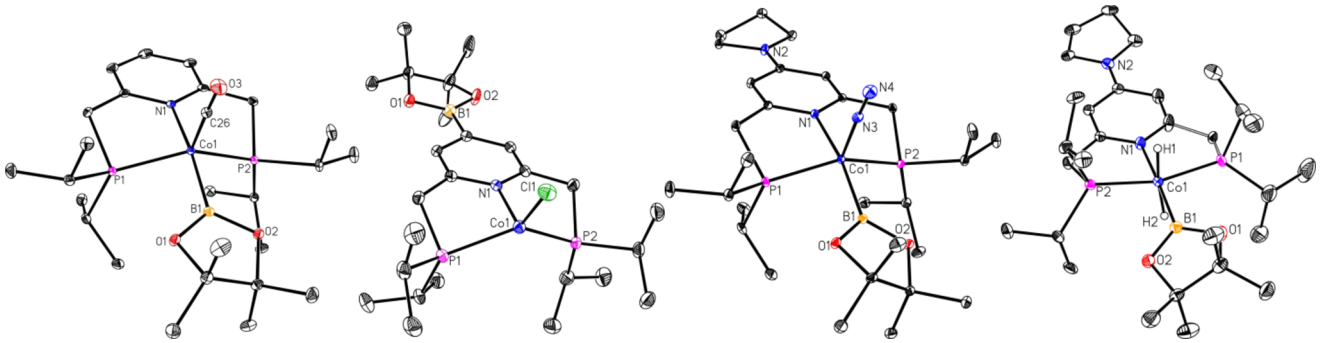

Figure 2. Solid state structures (from left to right) of **1-(CO)BPin**, **2-Cl**, **4-(N_2)BPin**, and **4-$(H)_2$BPin** at 30% probability ellipsoids. Hydrogen atoms, except the cobalt-hydrides omitted for clarity.

Scheme 4. Proposed Mechanism for the Cobalt-Catalyzed Borylation of Arenes with B_2Pin_2 and Solid State Structure of 2-$(H)_2$BPin (Resting State 2)

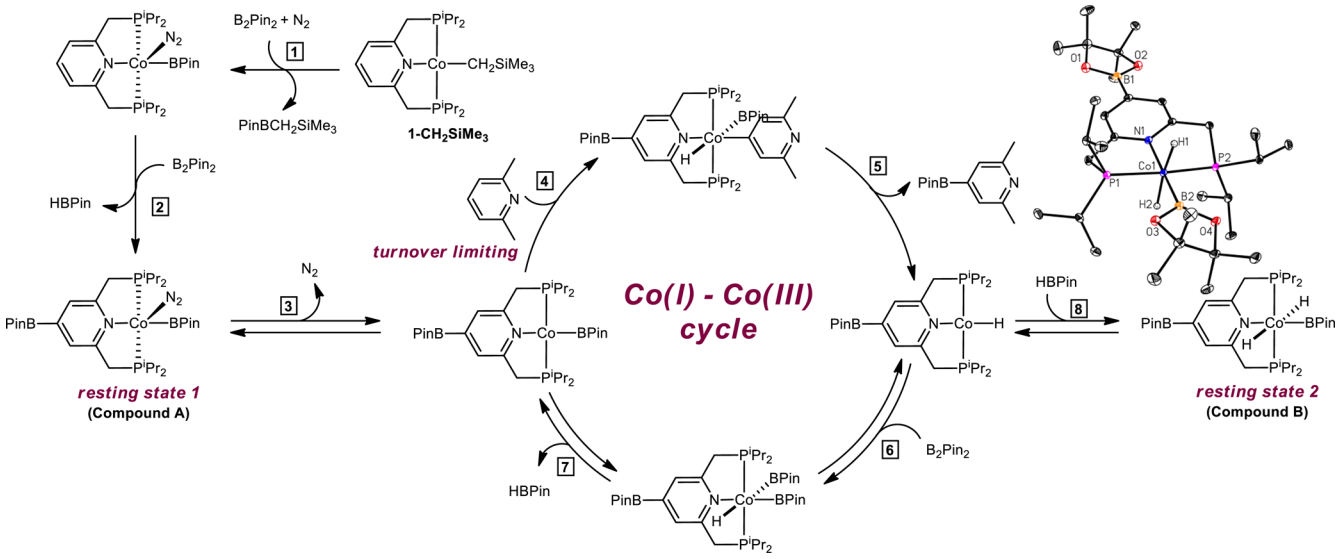

oxidative addition of HBPin to generate catalyst resting state 2, **2-$(H)_2$BPin** (step 8).

There are several important features of the proposed catalytic cycle:

(1) The cobalt-catalyzed borylation reaction operates via a Co(I)−Co(III) redox couple, where the oxidative addition and reductive elimination events are purely metal based and likely do not involve the metal and the ligand acting in concert via ligand aromatization-dearomatization.[26,27] Accessing d^8 and d^6 intermediates is distinct from the well-studied iridium catalysts where an Ir(III)−Ir(V) cycle is operative.[11]

(2) C−H borylation of the 4-position of the pyridine occurs in the cobalt catalyst, likely through a bimolecular process, before the borylation of the arene substrate, demonstrating the increased reactivity of this C−H bond compared to the 2,6-lutidine substrate that is present in vast excess.

(3) A cobalt(I)-boryl complex promotes oxidative addition of the C−H bond of the arene substrate.

(4) At early conversions, the catalyst resting state is the N_2-ligated cobalt(I)-boryl compound, **2-(N_2)BPin**, at 23 °C. At higher conversions and hence high concentrations of HBPin, the catalyst resting state is the cobalt(III) complex, **2-$(H)_2$BPin**.[28]

(5) The turnover-limiting step of the catalytic cycle using this specific cobalt catalyst is C−H oxidative addition, similar to what is observed with iridium.[11]

(6) Oxidative addition of B_2Pin_2 to a cobalt(I) hydride (step 6) and reductive elimination of HBPin from a cobalt(III) diboryl hydride species (step 7) are likely reversible. This claim is supported by the stoichiometric reaction of **2-(N_2)BPin** with excess HBPin (Scheme 3). The outcome of which yielded **2-$(H)_2$BPin** and B_2Pin_2, presumably via oxidative addition of HBPin to **2-BPin** (reverse of step 7) and then reductive elimination of B_2Pin_2 to form **2-H** (reverse of step 6). Subsequent oxidative addition of HBPin to **2-H** then yields the observed product, **2-$(H)_2$BPin**.[28]

Understanding the Influence of Substituents on the Electronic Properties of the PNP Pincer. The discovery that the borylation of the cobalt catalyst occurs faster than borylation of 2,6-lutidine raised the question of whether this modification is advantageous or deleterious to overall catalyst performance; understanding this effect is important for future catalyst design. To explore this effect, a series of substituted (PNP) cobalt complexes were synthesized (Scheme 5). The cobalt dichlorides were isolated following straightforward addition of the free pincer to a THF slurry of $CoCl_2$. Treatment of these compounds with one equivalent of $NaBEt_3H$ yielded the corresponding chlorides, **1-Cl**, **3-Cl**, **4-**

DOI: 10.1021/jacs.6b06144
J. Am. Chem. Soc. 2016, 138, 10645−10653

Scheme 5. Synthesis of Substituted (^{iPr}PNP) Cobalt Complexes[a]

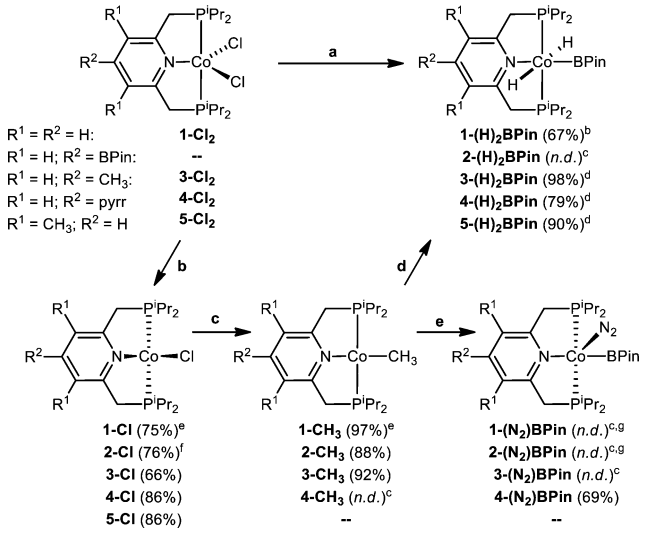

[a]Conditions (see S32 for complete experimental details): (a) 2 equiv $NaHBEt_3$, 2 or 4 equiv HBPin. (b) 1 equiv $NaHBEt_3$. (c) 1 equiv $LiCH_3$. (d) 2 equiv HBPin. (e) 1 equiv B_2Pin_2. [b]See ref 22. [c]Vacuum unstable and was not isolated on a preparative scale. [d]Yield using conditions (a). [e]See ref 25. [f]Prepared via the C−H borylation of **1-Cl** (see page S32). [g]See Scheme 3. *n.d.* = not determined.

Cl, and **5-Cl** in 75%, 66%, 86%, and 86% yields, respectively (step b). The BPin-substituted variant, **2-Cl**, was obtained in 76% yield following C−H borylation of **1-Cl** with **4-(H)$_2$BPin** and B_2Pin_2 (see S32). Cooling a concentrated 1:5 toluene/pentane solution of **2-Cl** to −35 °C produced bright green crystals suitable for X-ray diffraction (see Figure 2). The N_{py}−Co-Cl and P−Co−P angles of 118.72(11)° and 127.34(6)°, respectively, in the solid state structure of **2-Cl** established a near tetrahedral geometry, similar to what was observed in **1-Cl**.[25] The ^{1}H NMR spectrum of **2-Cl** in benzene-d_6 displayed broad paramagnetically shifted resonances. A solid-state magnetic moment (Gouy balance) of 2.5 μ_B was measured at 23 °C, consistent with a tetrahedral, high spin S = 1 complex.

The cobalt monomethyl compounds were prepared from addition of 1 equiv of $LiCH_3$ to the corresponding monochlorides (step c) to furnish **1-CH$_3$**, **2-CH$_3$**, and **3-CH$_3$** as diamagnetic solids in 97%, 88%, and 92% yields, respectively. Addition of 1 equiv of B_2Pin_2 to the cobalt monomethyl compounds under an N_2 atmosphere produced the corresponding cobalt boryl nitrogen compounds (step e). **1-(N$_2$)BPin**, **2-(N$_2$)BPin**, and **3-(N$_2$)BPin** were unstable to vacuum, thus precluding their isolation in the solid state. The pyrollidinyl-substituted variant, **4-(N$_2$)BPin**, however, was vacuum-stable and was isolated as a red powder in 69% yield and its solid state structure was determined by X-ray diffraction (Figure 2). The geometry about the cobalt is best described as pseudo-trigonal bipyramidal, with P−Co−P and N_{py}−Co-B angles of 141.635(17)° and 164.99(6)°, respectively. The dinitrogen and phosphine ligands occupy equatorial positions and the boryl and pyridine ligands define the axial positions, similar to what was observed in **1-(CO)BPin**. Treatment of the cobalt monomethyl compounds with 2 equiv of HBPin yielded the corresponding *trans*-dihydride boryl cobalt(III) compounds[22] (step d). A more straightforward route to these compounds was discovered where two equivalents of $NaHBEt_3$ were added to a stirring suspension of the cobalt dichloride along with 2 or 4 equiv of HBPin (step a). The resulting vacuum stable dihydride boryl compounds, **3-(H)$_2$BPin**, **4-(H)$_2$BPin**, and **5-(H)$_2$BPin** were obtained in 98%, 79% and 90% yields, respectively. The identity of **4-(H)$_2$BPin** was also confirmed by X-ray diffraction and a representation of the solid state structure is shown in Figure 2.

The electronic effect of introducing a substituent on the pincer ligand was assessed by cyclic voltammetry on the series of cobalt(I) monochlorides. This series of compounds was selected because all of the variants (**1-Cl**, **2-Cl**, **3-Cl**, **4-Cl**, and **5-Cl**) were vacuum stable and were obtained as analytically pure crystalline solids. The cyclic voltammograms recorded in THF solution are presented in Figure 3. The cobalt(I)

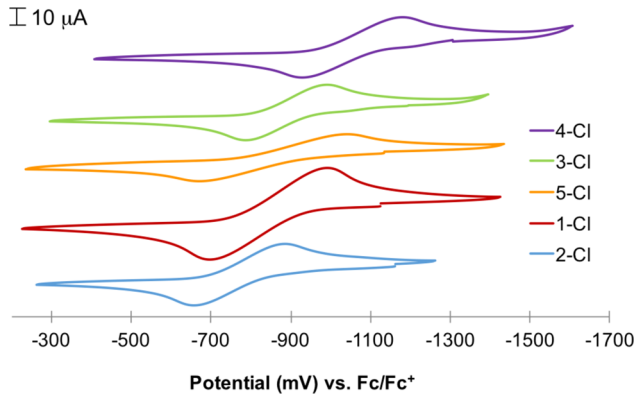

Figure 3. Cyclic voltammograms of **1-Cl**, **2-Cl**, **3-Cl**, **4-Cl**, and **5-Cl** in THF with 0.1 M $[NBu_4][PF_6]$ as the electrolyte as glassy carbon as the working electrode at 100 mV/s scan rate.

monochloride compounds display a single reversible wave, which we tentatively assign as the Co(I/II) redox couple,[14] and their measured redox potentials vs Fc/Fc^+ are reported in Table 1. The redox potentials become increasingly negative moving

Table 1. Measured Redox Potentials for Cobalt(I) Chloride Compounds

compound	substituent	$E°$ (mV vs Fc/Fc^+)
4-Cl	4-pyrr	−1050
3-Cl	4-Me	−877
5-Cl	3,5-Me	−850
1-Cl	4-H	−837
2-Cl	4-BPin	−770

from a 4-BPin to a 4-pyrr substituent, consistent with a more electron-rich metal center as electron donating groups are introduced into the 4-position.[29] Changing the 4-substituent from [H] to [BPin] shifts the redox potential by 67 mV, establishing a more electron-deficient metal center. Introduction of electron-donating groups shifts the reduction potential by −40 and −213 mV for Me and pyrr, respectively. Finally, introduction of methyl groups to the 3- and 5-positions of the pyridine slightly shifted the reduction potential of the parent compound by −13 mV, indicating that the cobalt is more electronically responsive to methylation on the 4-position of the pyridine ring rather than the 3- and 5-positions.

Evaluation of the Catalytic Activity of Substituted Cobalt Precatalysts. To determine the effect of pyridine substitution on catalytic C−H borylation activity, the time

DOI: 10.1021/jacs.6b06144
J. Am. Chem. Soc. 2016, 138, 10645−10653

course for the borylation of 2,6-lutidine with excess B_2Pin_2 using 15 mol % of various cobalt precatalysts was monitored by taking periodic aliquots from a cyclooctane solution (Figure 4).[30] The cobalt complex with the more electron-donating 4-

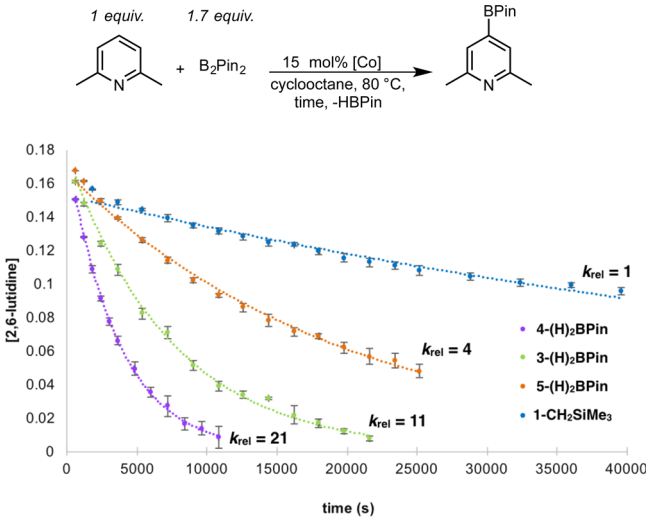

Figure 4. Reaction profiles for the C−H borylation of 2,6-lutidine with **4-(H)$_2$BPin** (purple), **3-(H)$_2$BPin** (green), **5-(H)$_2$BPin** (orange), and **1-CH$_2$SiMe$_3$** (blue) as precatalysts at 80 °C. [2,6-lutidine] was calculated from the GC yield of 4-BPin-2,6-dimethylpyridine using mesitylene as an internal standard. The reactions were performed under argon. Calculated k_{obs} values were obtained from the slope of ln[arene] vs time plots (see S55).

pyrr substituent (−213 mV difference by CV) was 21 times faster than the parent 4-H substituted compound, reaching complete conversion in less than 4 h at 80 °C. The rate acceleration with a more electron-rich catalyst is consistent with turnover-limiting C−H oxidative addition. The 4-Me and 3,5-Me substituted variants were faster than the parent catalyst (by 11 and 4 times, respectively) even though they have similar electronic properties (−40 mV and −13 mV, respectively). We attribute this rate difference to the observed borylation of **1-CH$_2$SiMe$_3$** prior to the borylation of the arene substrate, which shifts the redox potential of the corresponding monochloride by 67 mV, generating a less electron-rich and hence less active cobalt catalyst. These observations clearly demonstrate that borylation of the precatalyst under the reaction conditions has a detrimental effect on catalyst activity, presumably by slowing the rate of turnover limiting oxidative addition. The installation of an electron-donating group at the 4-position on the pincer not only increases electron density at the metal center, but also prevents catalyst inhibition by C−H borylation and introduction of an electron poor [BPin] substituent.

With more electron-donating precatalysts in hand, C−H borylation of electron-rich arenes in THF solution using equimolar amounts of arene and B_2Pin_2 was investigated. This is important from a practical perspective where more sophisticated arene substrates are too valuable to be used in excess. With the first generation precatalyst, **1-CH$_2$SiMe$_3$**, no detectable reaction was observed for the borylation of toluene under these conditions. With the more electron-rich and 4-position protected precatalysts, **3-(H)$_2$BPin** and **4-(H)$_2$BPin**, 27 and 34% conversion to products was observed (Table 2). With a more electron-rich arene, *m*-xylene, modest turnover was observed only with the most electron-rich precatalyst in the series, **4-(H)$_2$BPin** (Table 3).

Table 2. Evaluation of Different Cobalt Precatalysts in the Catalytic C−H Borylation of Toluene

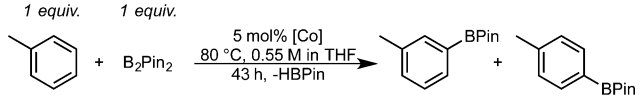

precatalyst	% conversion[a]	*m*:*p* ratio[b]
4-(H)$_2$BPin	34(3)%	69:31
3-(H)$_2$BPin	27(2)%	68:32
1-CH$_2$SiMe$_3$	<5%	N/A

[a]% Conversion with respect to toluene determined by GC analysis using mesitylene as internal standard. Reported number is the average of three experiments and the number in parentheses is the standard deviation. [b]*m*:*p* ratio is the average of three separate experiments determined by GC analysis without correcting for the small response factor variations between the two regioisomers.

Table 3. Evaluation of Various 4-Substituted PNP Cobalt Precatalysts for the Catalytic C−H Borylation of *m*-Xylene with B_2Pin_2

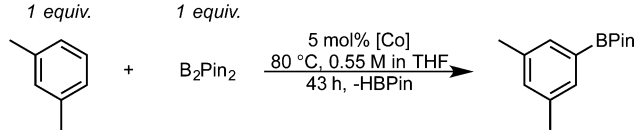

precatalyst	% yield[a]
4-(H)$_2$BPin	11(2)%
3-(H)$_2$BPin	<5%
1-CH$_2$SiMe$_3$	<5%

[a]%Conversion with respect to *m*-xylene determined by GC analysis using mesitylene as internal standard. Reported number is the average of 3 experiments and the number in parentheses is the standard deviation.

The catalytic results reported in Tables 2 and 3 highlight the advantage of the second generation, electron-rich catalysts. The 3,5-Me, 4-Me and the 4-pyrr catalysts exhibited 4-fold, 11-fold, and 21-fold rate enhancements, respectively, relative to the parent catalyst in the borylation of 2,6-lutidine. For the borylation of unactivated, electron-rich arenes such as toluene and *meta*-xylene in solvent using equimolar amounts of arene and B_2Pin_2, the first generation catalyst was completely ineffective, while the 4-Me and the 4-pyrr variants showed reasonable turnover, albeit in modest yields. These findings demonstrate that the more electron-rich 4-Me and the 4-pyrr variants not only displayed enhanced rates for the borylation of substrates that the first generation catalyst can already access, but also demonstrate that these rationally designed second generation catalysts can enable reactivity that is not possible with the first generation catalyst.

Kinetic Studies on 4-pyrr-(^{iPr}PNP)Co(H)$_2$BPin. Inspired by the improved activity of **4-(H)$_2$BPin**, additional studies were carried out to determine the origin of the rate acceleration. Monitoring the catalytic C−H borylation of 2,6-lutidine with B_2Pin_2 and 10 mol % of **4-(H)$_2$BPin** at 80 °C by ^{1}H and ^{31}P spectroscopy (at 23 °C) revealed similar behavior with **1-CH$_2$SiMe$_3$**. At early conversions (13% yield of product), **4-(N$_2$)BPin** was the only cobalt species observed by both ^{1}H and ^{31}P NMR spectroscopy. At higher conversions where there is a

DOI: 10.1021/jacs.6b06144
J. Am. Chem. Soc. 2016, 138, 10645−10653

higher concentration of HBPin (83% yield of product), the resting state shifts to **4-(H)$_2$BPin** (see S19).[31]

The experimental rate law for the borylation of 2,6-lutidine with B_2Pin_2 using **4-(H)$_2$BPin** as the precatalyst was also determined using the initial rates method (see S9) and by monitoring the reaction over 3−4 half-lives using excess B_2Pin_2 (see S11), similar to the study carried out by Hartwig and co-workers.[11] These data established the following overall rate equation:

$$\text{rate} = k_{obs}[\textbf{4-(H)}_2\textbf{BPin}]^1[\text{2, 6-lutidine}]^1[B_2Pin_2]^0 \quad (2)$$

A deuterium kinetic isotope effect was also measured (see S17) for the borylation of 2,6-lutidine and 4-*d*-2,6-lutidine at 80 °C in two separate vessels using the method of initial rates (up to 10% conversion). A normal primary KIE of 1.6(1) at 80 °C was observed. This KIE value close to unity suggests that the cleavage of the C−H bond in the borylation process does not occur in the turnover-limiting step. Taken together, these results are consistent with the interpretation that C−H activation is fast and reversible and the turnover-limiting step is C−B reductive elimination. The introduction of an electron-donating group that blocks borylation at the 4-position of the pincer lowers the barrier for C−H oxidative addition such that C−B reductive elimination becomes turnover limiting and the composite barrier is overall lower for more rapid turnover (Figure 5).

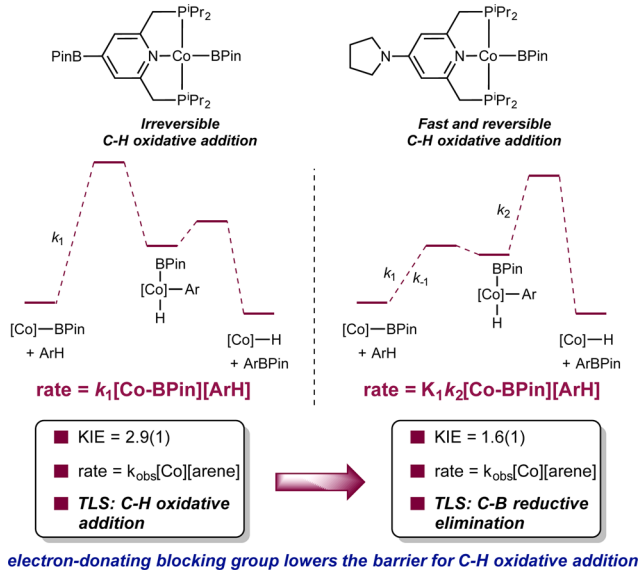

Figure 5. Qualitative, truncated reaction coordinate diagrams for **2-BPin** and **4-BPin** comparing the C−H oxidative addition and C−B reductive elimination steps in catalytic borylation. TLS = turnover-limiting step.

Nitrogen Inhibition Experiments. The catalyst resting states observed by ^{1}H and ^{31}P NMR spectroscopy at 23 °C at early conversions for both the first and second generation catalysts are cobalt dinitrogen boryl compounds, **2-(N$_2$)BPin** and **4-(N$_2$)BPin**. Although N_2 coordination to Co(I) is often weak, it is possible that dinitrogen could inhibit C−H activation and overall catalyst performance. To evaluate this possibility, the C−H borylation of 2,6-lutidine with excess B_2Pin_2 using 15 mol % of **4-(H)$_2$BPin**[32] was carried out under 3 different conditions (Figure 6): (i) under 1 atm of nitrogen, (ii) under argon (but not the solution was not degassed), and (iii) under

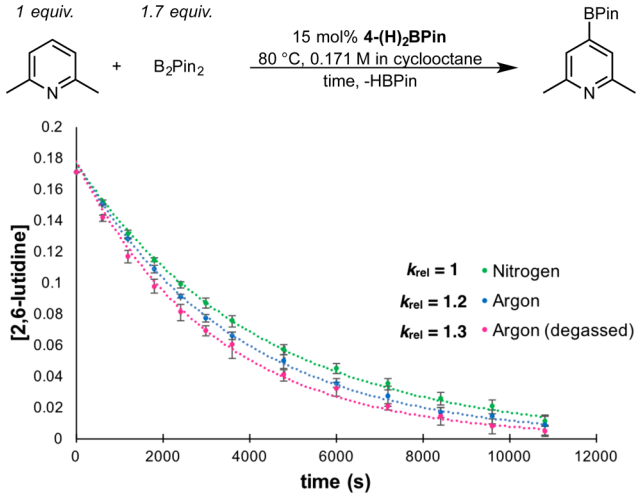

Figure 6. Reaction profiles for the C−H borylation of 2,6-lutidine with **4-(H)$_2$BPin** at 80 °C under nitrogen (green), argon (blue), and argon (degassed) (pink). [2,6-lutidine] was calculated from the GC yield of 4-BPin-2,6-dimethylpyridine using mesitylene as an internal standard. Calculated k_{obs} values were obtained from the slope of ln[arene] vs time plots (see S57).

argon where all solvents and reagents were rigorously degassed. The observed rate constant for each of these experiments is statistically indistinguishable (Figure 6), demonstrating no inhibitory role for dinitrogen. It is likely that at 80 °C, N_2 dissociation occurs to generate the four-coordinate cobalt(I) boryl, **4-BPin**. Both ^{1}H and ^{31}P NMR spectroscopic studies support rapid and reversible dinitrogen coordination. The spectra exhibit the number of peaks consistent with a C_{2v} rather than a C_s symmetric compound, indicating rapid dinitrogen dissociation and coordination at 23 °C. Warming the sample to 80 °C, resulted in a slight shifting of the resonances, also indicating perturbation of the equilibrium constant with increased concentration of the four-coordinate cobalt boryl (see S70). It is likely that at 80 °C, N_2 recoordination to **4-BPin** is slower than C−H activation and hence the lack of N_2 inhibition.

Synthesis of the Iridium Congener 4-pyrr-(^{iPr}PNP)Ir-(H)$_2$BPin and Evaluation of Catalytic Activity. The discovery that [(PNP)Co] catalysts promote catalytic C−H borylation by a Co(I)−Co(III) redox cycle raised the question if the corresponding iridium congeners would operate similarly. The iridium variant of the second-generation catalyst, **6-(H)$_2$BPin** was synthesized as shown in Scheme 6. Addition of the free pincer to $[Ir(COE)_2Cl]_2$ in the presence of excess HBPin yielded **6-(H)(Cl)BPin** as yellow powder in 76% yield. Subsequent treatment of this compound with $NaHBEt_3$

Scheme 6. Synthesis of 4-Pyrr-(^{iPr}PNP) Iridium Compounds[a]

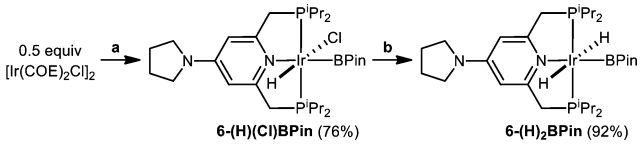

[a]Conditions (see S59 for full experimental details): (a) 1 equiv 4-pyrr-(^{iPr}PNP), 10 equiv HBPin. (b) 1 equiv $NaHBEt_3$.

DOI: 10.1021/jacs.6b06144
J. Am. Chem. Soc. 2016, 138, 10645−10653

resulted in isolation of **6-(H)$_2$BPin** in 92% yield as a light yellow powder (Scheme 6).

Cooling concentrated THF solutions of **6-(H)(Cl)BPin** and **6-(H)$_2$BPin** at −35 °C furnished crystals suitable for X-ray diffraction (Figure 7). The ^{31}P NMR spectrum of **6-(H)$_2$BPin**

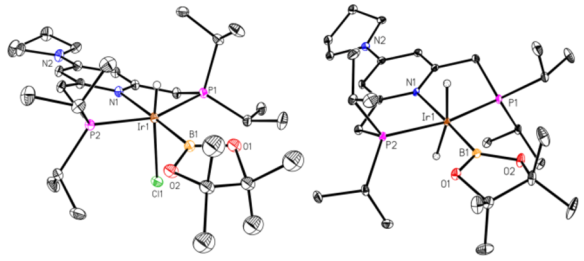

Figure 7. Solid state structures of **6-(H)(Cl)BPin** (left) and **6-(H)$_2$BPin** (right) at 30% probability ellipsoids. Hydrogen atoms, except the cobalt-hydrides omitted for clarity.

in THF-d_8 exhibited a sharp singlet at 55.60 ppm, in contrast to its cobalt congener, **4-(H)$_2$BPin**, where a broad singlet at 103.93 ppm was observed. This suggests that a dynamic process may be operative for cobalt, but not with iridium. Evaluation of **6-(H)$_2$BPin** for catalytic C−H borylation of 2,6-lutidine with B_2Pin_2 using 3 mol % of Ir produced no turnover (<5% conversion) after 24 h at 80 °C. Monitoring a THF-d_8 solution of the reaction mixture by ^{31}P NMR spectroscopy revealed **6-(H)$_2$BPin** as the iridium species present in highest concentration (see Figure S27), supporting a high barrier for H_2 reductive elimination preventing access to the putative iridium(I)-boryl.[33] This result highlights a fundamental difference between first and third row transition metals, namely that reductive elimination from octahedral, d^6 cobalt(III) is more facile than octahedral, d^6 iridium(III). While the mechanism for reductive elimination from these compounds remains under investigation and may involve phosphine dissociation to access a 5-coordinate intermediate,[34] the barrier for Ir(III)[35] is indisputably higher and suggests why Ir(V) compounds with bidentate ligands are preferred for catalytic C−H borylation.

CONCLUSIONS

The isolation of catalytic intermediates, stoichiometric experiments, and kinetic measurements provided valuable insights into the mechanism of turnover in cobalt-catalyzed C−H borylation. Our studies revealed that the catalytic cycle operates via a Co(I)−Co(III) redox couple where the C−H activating species is a cobalt(I) boryl intermediate and the turnover-limiting step is C−H oxidative addition of the arene. Borylation of the catalyst occurred prior to substrate functionalization and was found to have a deleterious effect on the catalytic performance by rendering the metal center less electron-rich, thus inhibiting oxidative addition. The results of our mechanistic studies inspired the rational design and synthesis of a more active 4-pyrrolidinyl substituted precatalyst, where the appended 4-pyrrolidinyl group served both as an electron-donating group and as a blocking group to prevent catalyst borylation. The iridium congener proved ineffective for catalytic C−H borylation due to a high barrier for reductive elimination from Ir(III), highlighting fundamental differences in catalyst design principles between first and third row transition metals.

ASSOCIATED CONTENT

Supporting Information

The Supporting Information is available free of charge on the ACS Publications website at DOI: 10.1021/jacs.6b06144.

Complete experimental details and characterization data of cobalt compounds (PDF)

Crystallographic data for **1-(CO)BPin**, **2-Cl**, **2-(H)$_2$BPin**, **4-(N$_2$)BPin**, **4-(H)$_2$BPin**, **6-(H)(Cl)BPin**, and **6-(H)$_2$BPin** (CIF)

AUTHOR INFORMATION

Corresponding Author

*pchirik@princeton.edu

Notes

The authors declare the following competing financial interest(s): J.V.O., S.P.S., and P.J.C. are inventors on U.S. Patent Application 61/913,522.

ACKNOWLEDGMENTS

We thank Princeton University for financial support. J.V.O. acknowledges the 2015 Howard Hughes Medical Institute International Student Research Fellowship, the 2014-2015 Bristol-Myers Squibb Graduate Fellowship in Synthetic Organic Chemistry, and the Paul Maeder '75 Fund for Energy and the Environment through the Andlinger Center for Energy and the Environment. We also thank AllyChem for a generous gift of B_2Pin_2, Dr. Valerie Schmidt for valuable suggestions in ligand synthesis, and Máté Bezdek for solving the X-ray structures of **6-(H)(Cl)BPin** and **6-(H)$_2$BPin**. We also thank the reviewers for their insightful comments and helpful suggestions to improve the manuscript.

REFERENCES

(1) For selected recent reviews see: (a) Daugulis, O.; Do, H.-Q.; Shabashov. *Acc. Chem. Res.* **2009**, *42*, 1074. (b) Chen, X.; Engle, K. M.; Wang, D.-H.; Yu, J.-Q. *Angew. Chem., Int. Ed.* **2009**, *48*, 5094. (c) Ackermann, R.; Vicente, R.; Kapdi, A. R. *Angew. Chem., Int. Ed.* **2009**, *48*, 9792. (d) Colby, D. A.; Bergman, R. G.; Ellman, J. A. *Chem. Rev.* **2010**, *110*, 624. (e) Gutekunst, W. R.; Baran, P. S. *Chem. Soc. Rev.* **2011**, *40*, 1976. (f) Arockiam, P. B.; Bruneau, C.; Dixneuf, P. H. *Chem. Rev.* **2012**, *112*, 5879. (g) Neufeldt, S. R.; Sanford, M. S. *Acc. Chem. Res.* **2012**, *45*, 936. (h) Li, B.-J.; Shi, Z.-J. *Chem. Soc. Rev.* **2012**, *41*, 5588. (i) Mousseau, J.; Charette, A. B. *Acc. Chem. Res.* **2013**, *46*, 412.

(2) (a) Ishiyama, T.; Miyaura, N. *Pure Appl. Chem.* **2006**, *78*, 1369. (b) Mkhalid, I. A. I.; Barnard, J. H.; Marder, T. B.; Murphy, J. M.; Hartwig, J. F. *Chem. Rev.* **2010**, *110*, 890. (c) Hartwig, J. F. *Acc. Chem. Res.* **2012**, *45*, 864. (d) Metal-free catalytic C-H borylation has also been reported using FLP catalysis, see: Légaré, M.; Courtemanche, M.; Rochette, E.; Fontaine, F. *Science* **2015**, *349*, 513.

(3) Johansson Seechurn, C. C. C.; Kitching, M. O.; Colacot, T. J.; Snieckus, V. *Angew. Chem., Int. Ed.* **2012**, *51*, 5062.

(4) Hall, D. G. *Boronic Acids*; Wiley-VCH: Weinheim, Germany, 2005.

(5) Cho, J.−Y.; Tse, M. K.; Holmes, D.; Maleczka, R. E., Jr.; Smith, M. R., III *Science* **2002**, *295*, 305.

(6) Ishiyama, T.; Takagi, J.; Ishida, K.; Miyaura, N.; Anastasi, N. R.; Hartwig, J. F. *J. Am. Chem. Soc.* **2002**, *124*, 390.

(7) Preshlock, S. M.; Ghaffari, B.; Maligres, P. E.; Krska, S. W.; Maleczka, R. E.; Smith, M. R. *J. Am. Chem. Soc.* **2013**, *135*, 7572.

(8) Larsen, M. A.; Hartwig, J. F. *J. Am. Chem. Soc.* **2014**, *136*, 4287.

(9) Maleczka, R. E., Jr.; Shi, F.; Holmes, D.; Smith, M. R., III *J. Am. Chem. Soc.* **2003**, *125*, 7792. (b) Beck, E. M.; Hatley, R.; Gaunt, M. J. *Angew. Chem., Int. Ed.* **2008**, *47*, 3004. (c) Fischer, D. F.; Sarpong, R. *J. Am. Chem. Soc.* **2010**, *132*, 5926. (d) Liao, X.; Stanley, L. M.; Hartwig,

DOI: 10.1021/jacs.6b06144
J. Am. Chem. Soc. 2016, 138, 10645−10653

J. F. *J. Am. Chem. Soc.* **2011**, *133*, 2088. (e) Leal, R. A.; Beaudry, D. R.; Alzghari, S. K.; Sarpong, R. *Org. Lett.* **2012**, *14*, 5350. (f) Preshlock, S. M.; Plattner, D. L.; Maligres, P. E.; Krska, S. W.; Maleczka, R. E.; Smith, M. R. *Angew. Chem., Int. Ed.* **2013**, *52*, 12915. (g) Han, S.; Morrison, K. C.; Hergenrother, P. J.; Movassaghi, M. *J. Org. Chem.* **2014**, *79*, 473.

(10) Kawamorita, S.; Miyazaki, T.; Ohmiya, H.; Iwai, T.; Sawamura, M. *J. Am. Chem. Soc.* **2011**, *133*, 19310. (b) Kawamorita, S.; Miyazaki, T.; Iwai, T.; Ohmiya, H.; Sawamura, M. *J. Am. Chem. Soc.* **2012**, *134*, 12924. (c) Kawamorita, S.; Miyazaki, T.; Ohmiya, H.; Iwai, T.; Sawamura, M. *J. Am. Chem. Soc.* **2011**, *133*, 19310.

(11) Boller, T. M.; Murphy, J. M.; Hapke, M.; Ishiyama, T.; Miyaura, N.; Hartwig, J. F. *J. Am. Chem. Soc.* **2005**, *127*, 14263.

(12) (a) Tamura, H.; Yamazaki, H.; Sato, H.; Sakaki, S. *J. Am. Chem. Soc.* **2003**, *125*, 16114. (b) Green, A. G.; Liu, P.; Merlic, C. A.; Houk, K. N. *J. Am. Chem. Soc.* **2014**, *136*, 4575.

(13) Mankad, N. P. *Synlett* **2014**, *25*, 1197.

(14) Semproni, S. P.; Milsmann, C.; Chirik, P. J. *J. Am. Chem. Soc.* **2014**, *136*, 9211.

(15) Waltz, K. M.; He, W.; Muhoro, C.; Hartwig, J. F. *J. Am. Chem. Soc.* **1995**, *117*, 11357.

(16) Mazzacano, T. J.; Mankad, N. P. *J. Am. Chem. Soc.* **2013**, *135*, 17258.

(17) Mazzacano, T. J.; Mankad, N. P. *Chem. Commun.* **2015**, *51*, 5379.

(18) Hatanaka, T.; Ohki, Y.; Tatsumi, K. *Chem. - Asian J.* **2010**, *5*, 1657.

(19) Dombray, T.; Werncke, C. G.; Jiang, S.; Grellier, M.; Vendier, L.; Bontemps, S.; Sortais, J.; Sabo-Etienne, S.; Darcel, C. *J. Am. Chem. Soc.* **2015**, *137*, 4062.

(20) Yan, G.; Jiang, Y.; Kuang, C.; Wang, S.; Liu, H.; Zhang, Y.; Wang, J. *Chem. Commun.* **2010**, *46*, 3170.

(21) (a) Furukawa, T.; Tobisu, M.; Chatani, N. *Chem. Commun.* **2015**, *51*, 6508. (b) Zhang, H.; Hagihara, S.; Itami, K. *Chem. Lett.* **2015**, *44*, 779.

(22) Obligacion, J. V.; Semproni, S. P.; Chirik, P. J. *J. Am. Chem. Soc.* **2014**, *136*, 4133.

(23) Schaefer, B. A.; Margulieux, G. W.; Small, B. L.; Chirik, P. J. *Organometallics* **2015**, *34*, 1307.

(24) Khaskin, E.; Diskin-Posner, Y.; Weiner, L.; Leitus, G.; Milstein, D. *Chem. Commun.* **2013**, *49*, 2771.

(25) Semproni, S. P.; Atienza, C. C. H.; Chirik, P. J. *Chem. Sci.* **2014**, *5*, 1956.

(26) Ben-Ari, E.; Leitus, G.; Shimon, L. J. W.; Milstein, D. *J. Am. Chem. Soc.* **2006**, *128*, 15390.

(27) Addition of DBPin to a benzene-d_6 solution of **4-(H)$_2$BPin** resulted in immediate isotopic exchange in the cobalt-hydride(deuteride) positions (see page S63). Also, addition of B_2Pin_2 to a benzene-d_6 solution of **4-(H)$_2$BPin** furnished **4-(H$_2$/D$_2$/HD)BPin** arising from the borylation of benzene-d_6 and the residual natural abundance arene (see page S65). No isotopic label was incorporated in the pincer under both of these conditions. These results are consistent with oxidative addition-reductive elimination of B-H(D) as well as C-H(D) bonds through a metal-based redox cycle rather than metal−ligand cooperativity involving reversible ligand dearomatization-aromatization (ref 26).

(28) An equilibrium constant of 0.52 was calculated for the interconversion of **2-BPin** and **2-(H)$_2$BPin** (see S27). The formation of B_2Pin_2 and H_2 from 2 equivalents of HBPin is thermodynamically unfavorable (~12 kcal/mol uphill; see ref 2b). The formation of **2-(H)$_2$BPin** and B_2Pin_2 from **2-BPin** and HBPin is most likely driven by the formation of 2 cobalt-hydride bonds in **2-(H)$_2$BPin**.

(29) (a) A similar study probing the effect of the 4-substituent on a PNP pincer ligand was also investigated for dinitrogen reduction: see Kuriyama, S.; Arashiba, K.; Nakajima, K.; Tanaka, H.; Kamaru, N.; Yoshizawa, K.; Nishibayashi, Y. *J. Am. Chem. Soc.* **2014**, *136*, 9719. (b) Electron-donating groups on the 4- and 4′-positions of 2,2′-bipyridine was shown to improve C−H borylation activity: see Ishiyama, T.; Takagi, J.; Hartwig, J. F.; Miyaura, N. *Angew. Chem., Int. Ed.* **2002**, *41*, 3056.

(30) Attempts to monitor the reaction profiles of the borylation of 1,3-bis(trifluoromethyl)benzene with B_2Pin_2 using the different cobalt precatalysts using identical conditions were unsuccessful due to the high rates of these reactions (complete conversion in 6 min for all the precatalysts).

(31) An equilibrium constant of 3.02 was calculated for the interconversion of **4-BPin** and **4-(H)$_2$BPin** (see S52). See ref 28.

(32) The cobalt precursor, **4-(H)$_2$BPin**, was selected for N_2 inhibition experiments due to its relative ease of isolation and ability to measure the effect of vacuum on the rate cobalt-catalyzed C-H borylation as **4-(N$_2$)BPin** cannot be isolated in the absence of dinitrogen. Under catalytic conditions, **4-(H)$_2$BPin** is immediately and quantitatively converted to **4-(N$_2$)BPin** before any product is observed (see the red ^{31}P NMR spectrum on Figure S9). In these experiments and in the presence of N_2, the starting cobalt complex before heating and degassing is **4-(N$_2$)BPin** and not **4-(H)$_2$BPin**.

(33) Addition of DBPin to a THF-d_8 solution of **6-(H)$_2$BPin** resulted to no isotopic exchange in the hydride (deuteride) position, indicating that reductive elimination does not occur these conditions (see S67).

(34) (a) Crumpton, D. M.; Goldberg, K. I. *J. Am. Chem. Soc.* **2000**, *122*, 962. (b) Xu, H.; Bernskoetter, W. H. *J. Am. Chem. Soc.* **2011**, *133*, 14956.

(35) The reluctance of Ir(III) compounds with a bidentate ligand to undergo reductive elimination was first proposed by Sakaki and co-workers (ref 12a).

DOI: 10.1021/jacs.6b06144
J. Am. Chem. Soc. 2016, 138, 10645−10653